Since January 2020 Elsevier has created a COVID-19 resource centre with free information in English and Mandarin on the novel coronavirus COVID-19. The COVID-19 resource centre is hosted on Elsevier Connect, the company's public news and information website.

Microbial Risk Analysis 24 (2023) 100263

Contents lists available at ScienceDirect

Microbial Risk Analysis

journal homepage: www.elsevier.com/locate/mran

Ghosts of the past: Elemental composition, biosynthesis reactions and thermodynamic properties of Zeta P.2, Eta B.1.525, Theta P.3, Kappa B.1.617.1, Iota B.1.526, Lambda C.37 and Mu B.1.621 variants of SARS-CoV-2

Marko Popovic [a,*], Marijana Pantović Pavlović [a,b], Miroslav Pavlović [a,b]

[a] Institute of Chemistry, Technology and Metallurgy, University of Belgrade, Njegoševa 12, 11000 Belgrade, Serbia
[b] University of Belgrade, Centre of Excellence in Chemistry and Environmental Engineering - ICTM, Belgrade, Serbia

ARTICLE INFO

Keywords:
Enthalpy
Entropy
Gibbs energy
Bioenergetics
Biothermodynamics
Evolution

ABSTRACT

From the perspectives of molecular biology, genetics and biothermodynamics, SARS-CoV-2 is the among the best characterized viruses. Research on SARS-CoV-2 has shed a new light onto driving forces and molecular mechanisms of viral evolution. This paper reports results on empirical formulas, biosynthesis reactions and thermodynamic properties of biosynthesis (multiplication) for the Zeta P.2, Eta B.1.525, Theta P.3, Kappa B.1.617.1, Iota B.1.526, Lambda C.37 and Mu B.1.621 variants of SARS-CoV-2. Thermodynamic analysis has shown that the physical driving forces for evolution of SARS-CoV-2 are Gibbs energy of biosynthesis and Gibbs energy of binding. The driving forces have led SARS-CoV-2 through the evolution process from the original Hu-1 to the newest variants in accordance with the expectations of the evolution theory.

1. Introduction

The COVID-19 pandemic has started in late 2019 [Wu et al., 2020; CDC, 2023]. The cause of the disease was found to be SARS-CoV-2, which was later labeled the Hu-1 variant [Pavan et al., 2022]. The SARS-CoV-2 genome has passed through several dozen mutations, during 2020, 2021 and 2022. Mutations have caused the appearance of new variants, some of which have caused pandemic waves. This has led to suppression of the older variants and domination of the mutants. Since the beginning of the pandemic, globally, as of 6:21pm CET, 7 March 2023, there have been 759,408,703 confirmed cases of COVID-19, including 6,866,434 deaths, reported to WHO [2023a].

Morphology of SARS-CoV-2 is known [Riedel et al., 2019]. The sequence of nucleotides of the majority of variants of SARS-CoV-2 has been reported [Khare et al., 2021; Elbe and Buckland-Merrett, 2017; Shu and McCauley, 2017; GISAID, 2023; Sayers et al., 2022; NCBI, 2023]. The protein sequences have also been reported [Sayers et al., 2022; NCBI, 2023; The UniProt Consortium, 2023; UniProt, 2023; Coudert et al., 2023; Wang et al., 2021]. Empirical formulas for most variants of SARS-CoV-2 have been reported [Degueldre, 2021; Şimşek et al., 2021; Popovic and Minceva, 2020b; Popovic, 2023a, 2023b, 2023c, 2022b, 2022c, 2022d, 2022e]. The empirical formulas have been determined using the atom counting method [Popovic, 2022a]. Şimşek et al. [2021] used a computational method that resembles the atom counting method [Popovic, 2022a; Popovic and Minceva, 2020b]. Thermodynamic properties for most SARS-CoV-2 variants have been reported [Gale, 2022; Şimşek et al., 2021; Popovic and Minceva, 2020b, 2021a; Popovic and Popovic, 2022; Popovic, 2023a, 2023b, 2023c, 2022b, 2022c, 2022d, 2022e, 2022f, 2022g, 2022h]. However, empirical formulas and thermodynamic properties have never been determined for the Zeta P.2, Eta B.1.525, Theta P.3, Kappa B.1.617.1, Iota B.1.526, Lambda C.37 and Mu B.1.621 variants of SARS-CoV-2. Knowing these data is needed to accurately follow the chemical and thermodynamic background of time evolution of SARS-CoV-2.

The mechanistic model of interactions of SARS-CoV-2 with its host has been reported in [Gale, 2022; Zhang et al., 2021, 2022; Xie et al., 2020; Jackson et al., 2022; Overduin et al., 2022; Popovic and Minceva, 2020b; Popovic and Popovic, 2022; Popovic, 2022e]. The competition between different variants of SARS-CoV-2 and different other viruses has been reported in the literature [Popovic and Minceva, 2021a; Popovic, 2023a, 2023b, 2023c].

SARS-CoV-2 belongs to RNA viruses, which exhibit a great tendency

* Corresponding author.
E-mail address: marko.popovic@ihtm.bg.ac.rs (M. Popovic).

https://doi.org/10.1016/j.mran.2023.100263
Received 26 March 2023; Received in revised form 7 May 2023; Accepted 19 May 2023
Available online 20 May 2023

towards mutation [Duffy, 2018]. Mutations on SARS-CoV-2 are so common that even though chemical composition and thermodynamic properties have been reported for most SARS-CoV-2 variants, until now they have not been reported for multiple variants. Accumulation of mutations in SARS-CoV-2 enables to follow the time evolution of the virus.

Subcellular and cellular microorganisms represent open thermodynamic systems [von Bertalanffy, 1950, 1971; von Stockar, 2013a, 2013b; Assael et al., 2022; Popovic, 2018]. Thus, biothermodynamics and bioenergetics have proved themselves excellent tools in analysis of growth and other metabolic processes performed by microorganisms [von Stockar, 2013a, 2013b; Assael et al., 2022]. Schrödinger used the entropy concept to provide the first ever physical definition of life [Schrödinger, 1944]. The second law has been applied by Morowitz to analyze biological order, metabolism and the origin of life [Morowitz et al., 2000, 1988; Morowitz, 1995, 1992, 1968, 1955]. The full potential of thermodynamics in life sciences was achieved with the development of nonequilibrium thermodynamics by Prigogine [Prigogine, 1977, 1947; Prigogine and Wiame, 1946; Glansdorff and Prigogine, 1971; Popovic, 2018; Müller, 2010].

The first step in biothermodynamic analysis is to determine the elemental composition and thermodynamic properties of microorganisms [Battley, 1999a, 1999b, 1992; Assael et al., 2022]. Empirical formulas and thermodynamic properties have been determined for many microorganism species, both cellular [Battley et al., 1997; Battley, 1999a, 1999b, 1992; Duboc et al., 1999; Popovic, 2019; Popovic et al., 2021] and subcellular [Şimşek et al., 2021; Gale, 2022, 2020, 2019, 2018; Popovic, 2022e]. The next step is to construct biosynthesis reactions that describe conversion of nutrients into new live matter and find thermodynamic properties of biosynthesis [Battley, 2013, 1999b; Assael et al., 2022].

Biothermodynamics has also been used to analyze the process of biological evolution by Hansen et al. [2021, 2018, 2009] and Skene [2015]. Virus-host interactions have been discussed for different viruses: Rhinovirus [Casasnovas and Springer, 1995], arboviruses [Gale, 2020, 2019], HIV [Gale, 2020], Ebola virus [Popovic, 2022i], MPXV [Popovic, 2022j], vaccinia [Popovic, 2022j], bacteriophages [Popovic, 2023d] and viroids [Popovic, 2023e]. Thermodynamic properties for the human host tissues have been reported [Popovic and Minceva, 2020c; Popovic, 2023f, 2022i].

The goal of this paper is to shed more light on elemental composition, growth reactions and thermodynamic properties for Zeta P.2, Eta B.1.525, Theta P.3, Kappa B.1.617.1, Iota B.1.526, Lambda C.37 and Mu B.1.621 variants of SARS-CoV-2, which have not been reported until now. Knowing thermodynamic properties of all the variants should provide more insights on the thermodynamic background of evolution of SARS-CoV-2.

2. Methods

2.1. Data sources

Genetic sequences of isolates of the Zeta P.2, Eta B.1.525, Theta P.3, Kappa B.1.617.1, Iota B.1.526, Lambda C.37 and Mu B.1.621 variants of SARS-CoV-2, were taken from GISAID, the global data science initiative [Khare et al., 2021; Elbe and Buckland-Merrett, 2017; Shu and McCauley, 2017; GISAID, 2023]. The genetic sequence of the Zeta P.2 variant can be found under the accession code EPI_ISL_17074902 and is labeled hCoV-19/Brazil/SP-FIOCRUZ-34486/2020. It was isolated on November 23, 2020 in Sao Paulo. The genetic sequence of the Eta B.1.525 can be found under the accession code EPI_ISL_16347671 and is labeled hCoV-19/Hong Kong/HKU-188/2021. It was isolated on June 10, 2021 in Hong Kong. The genetic sequence of the Theta P.3 variant can be found under the accession code EPI_ISL_3353945 and is labeled hCoV-19/Guam/GU-CDC-2-3906074-/2021. It was isolated on January 31, 2021 in Guam. The genetic sequence of the Kappa B.1.617.1 variant can be found under the accession code EPI_ISL_2758215 and is labeled hCoV-19/India/un-IRSHA-CD210871/2020. It was isolated on March 3, 2020 in India. The genetic sequence of the Iota B.1.526 variant can be found under the accession code EPI_ISL_16100366 and is labeled hCoV-19/USA/RI-RISHL-D00486/2021. It was isolated on February 22, 2021 in USA. The genetic sequence of the Lambda C.37 variant can be found under the accession code EPI_ISL_16027351 and is labeled hCoV-19/Panama/CDED13928-GMI/2021. It was isolated on April 15, 2021 in Panama. The genetic sequence of the Mu B.1.621 variant can be found under the accession code EPI_ISL_17028749 and is labeled hCoV-19/Chile/AN-ISPC-131692/2021. It was isolated on July 25, 2021 in Chile. Therefore, the findings of this study are based on metadata associated with 7 sequences available on GISAID up to March 17, 2023, and accessible at https://doi.org/10.55876/gis8.230317sf. More information about the genetic sequences can be found in the Supplementary Material.

The sequence of the nucleocapsid phosphoprotein of SARS-CoV-2 was obtained from the NCBI database [Sayers et al., 2022; NCBI, 2023], under the accession ID: UKQ14424.1. The number of copies of the nucleocapsid phosphoprotein in virus particle was taken from [Neuman and Buchmeier, 2016; Neuman et al., 2011; Neuman et al., 2006].

Data on WHO labels, lineages and additional mutations, countries of first detection, spike mutations of interest, and years and months of first detection for the Eta, Theta, Kappa, Iota, Zeta, Mu and Lambda variants of SARS-CoV-2 were taken from [ECDC, 2023].

2.2. Empirical formulas and biosynthesis reactions

The genetic and protein sequences were used to find empirical formulas of nucleocapsids of the BA.5.2 and BF.7 variants of SARS-CoV-2. This was done using the atom counting method [Popovic, 2022a]. The atom counting method is implemented using a computer program [Popovic, 2022a]. The input are viral genetic and protein sequences, as well as the number of copies of proteins in the virus particle and the virus particle size [Popovic, 2022a]. The program goes along the nucleic acid and protein sequences and adds atoms coming from each residue in the sequence, to find the number of atoms contributed by that macromolecule to the virus particle [Popovic, 2022a]. The contributions of viral proteins are multiplied by their copy numbers, since proteins are present in multiple copies in virus particles [Popovic, 2022a]. The output of the program is elemental composition of virus particles, in the form of empirical formulas, and molar masses of virus particles [Popovic, 2022a]. The advantage of the atom counting method is that it can provide the empirical formulas of virus particles, based on widely available data on genetic and protein sequences [Popovic, 2022a]. The atom counting method was shown to give results in good agreement with experimental results [Popovic, 2022a].

The empirical formulas of virus particles were used to construct biosynthesis reactions, summarizing conversion of nutrients into new live matter [von Stockar, 2013a, 2013b; Battley, 1998]. The biosynthesis reaction for virus particles has the general form

$$(\text{Aminoacid}) + O_2 + HPO_4^{2-} + HCO_3^- \rightarrow (\text{Bio}) + SO_4^{2-} + H_2O + H_2CO_3 \quad (1)$$

where (Bio) represents new live matter, described by an empirical formula given by the atom counting method [Popovic, 2023a, 2022b, 2022e]. (Amino acid) represents a mixture of amino acids with the empirical formula $CH_{1.798}O_{0.4831}N_{0.2247}S_{0.022472}$ (expressed per mole of carbon), representing the source of energy, carbon, nitrogen and sulfur [Popovic, 2023a, 2022b, 2022e]. O_2 is the electron acceptor [Popovic, 2023a, 2022b, 2022e]. HPO_4^{2-} is the source of phosphorus [Popovic, 2023a, 2022b, 2022e]. HCO_3^- is a part of the bicarbonate buffer that takes excess H^+ ions that are generated during biosynthesis [Popovic, 2023a, 2022b, 2022e]. SO_4^{2-} is an additional metabolic product that takes excess sulfur atoms [Popovic, 2023a, 2022b, 2022e]. H_2CO_3 takes

Table 1
Empirical formulas of nucleocapsids of SARS-CoV-2 variants. The empirical formulas have the general form $C_{nC}H_{nH}O_{nO}N_{nN}P_{nP}S_{nS}$, with the n_C, n_H, n_O, n_N, n_P and n_S coefficients from this table. The table also provides molar masses of empirical formulas, *Mr*, in g/C-mol (Da), as well as molar masses of entire nucleocapsids, *Mr*(*nc*), in MDa.

Namex	n_C	n_H	n_O	n_N	n_P	n_S	Mr (g/C-mol)	Mr(nc) (MDa)
Zeta P.2	1	1.573524	0.342720	0.312382	0.006034	0.003358	23.7501	117.228
Eta B.1.525	1	1.573539	0.342699	0.312381	0.006029	0.003358	23.7496	117.220
Theta P.3	1	1.573478	0.342775	0.312394	0.006047	0.003358	23.7514	117.251
Kappa B.1.617.1	1	1.573509	0.342742	0.312384	0.006038	0.003358	23.7505	117.235
Iota B.1.526	1	1.573526	0.342719	0.312381	0.006033	0.003358	23.7500	117.227
Lambda C.37	1	1.573499	0.342751	0.312387	0.006041	0.003358	23.7508	117.240
Mu B.1.621	1	1.573821	0.342372	0.312300	0.005948	0.003361	23.7410	117.081

the oxidized carbon atoms and is also a part of the bicarbonate buffer [Popovic, 2023a, 2022b, 2022e].

2.3. Thermodynamic properties of live matter and biosynthesis

Empirical formulas of virus nucleocapsids were used to find standard thermodynamic properties of their live matter, using predictive biothermodynamic models, i.e. Patel-Erickson and Battley equations [Patel and Erickson, 1981; Battley, 1999a, 1998, 1992; Battley and Stone, 2000]. The Patel-Erickson equation was used to find enthalpy of live matter, based on its elemental composition. The Patel-Erickson equation gives standard enthalpy of combustion, $\Delta_C H^o$, of live matter

$$\Delta_C H^0(bio) = -111.14 \frac{kJ}{C-mol} \cdot E \tag{2}$$

where E is number of electrons transferred to oxygen during combustion [Patel and Erickson, 1981; Battley, 1998, 1992]. E can be calculated from the empirical formula of live matter

$$E = 4n_C + n_H - 2n_O - 0\ n_N + 5n_P + 6n_S \tag{3}$$

where n_C, n_H, n_O, n_N, n_P and n_S represent the numbers of C, H, O, N, P and S atoms in the live matter empirical formula, respectively [Patel and Erickson, 1981; Battley, 1998, 1992]. Once calculated using the Patel-Erickson equation, $\Delta_C H^o$ can be converted into standard enthalpy of formation, $\Delta_f H^o$, of live matter. $\Delta_C H^o$ is the enthalpy change of the reaction of complete combustion of live matter.

This means that $\Delta_C H^o$ can be used to find $\Delta_f H^o$ of live matter using the equation [Popovic, 2023a, 2022b, 2022e; Atkins and de Paula, 2011, 2014]

$$C_{nC}H_{nH}O_{nO}N_{nN}P_{nP}S_{nS} + (n_C + 1/4n_H + 11/4n_P + 11/2n_S - 1/2n_O)O_2 \rightarrow n_C CO_2 + 1/2n_H H_2O + 1/2n_N N_2 + 1/4n_P P_4O_{10} + n_S SO_3 \tag{4}$$

$$\Delta_f H^0(bio) = n_C\ \Delta_f H^0(CO_2) + \frac{n_H}{2}\ \Delta_f H^0(H_2O) + \frac{n_P}{4}\ \Delta_f H^0(P_4O_{10}) + n_S\ \Delta_f H^0(SO_3) - \Delta_C H^0 \tag{5}$$

The Battley equation [Battley, 1999a; Battley and Stone, 2000] gives standard molar entropy of live matter, S^o_m, based on its empirical formula

$$S^0_m(bio) = 0.187 \sum_J \frac{S^0_m(J)}{a_J} n_J \tag{6}$$

where n_J is the number of atoms of element J in the empirical formula of live matter [Battley, 1999a; Battley and Stone, 2000]. S^o_m and a_J are standard molar entropy and number of atoms per formula unit of element J in its standard state elemental form [Battley, 1999a; Battley and Stone, 2000]. The Battley equation can be modified to give standard entropy of formation, $\Delta_f S^o$, of live matter [Battley, 1999a; Battley and Stone, 2000]

$$\Delta_f S^0(bio) = -0.813 \sum_J \frac{S^0_m(J)}{a_J} n_J \tag{7}$$

Finally, $\Delta_f H^o$ and $\Delta_f S^o$ are combined to give standard Gibbs energy of formation of live matter, $\Delta_f G^o$.

$$\Delta_f G^0(bio) = \Delta_f H^0(bio) - T\Delta_f S^0(bio) \tag{8}$$

Once live matter is characterized by finding its $\Delta_f H^o$, S^o_m and $\Delta_f G^o$, these properties can be combined with biosynthesis reactions to find standard thermodynamic properties of biosynthesis. Standard thermodynamic properties of biosynthesis include standard enthalpy of biosynthesis, $\Delta_{bs} H^o$, standard entropy of biosynthesis, $\Delta_{bs} S^o$, and standard Gibbs energy of biosynthesis, $\Delta_{bs} G^o$. These properties are found by applying the Hess's law to biosynthesis reactions

$$\Delta_{bs} H^0 = \sum_{products} \nu\ \Delta_f H^0 - \sum_{reactants} \nu\ \Delta_f H^0 \tag{9}$$

$$\Delta_{bs} S^0 = \sum_{products} \nu\ S^o_m - \sum_{reactants} \nu\ S^o_m \tag{10}$$

$$\Delta_{bs} G^0 = \sum_{products} \nu\ \Delta_f G^0 - \sum_{reactants} \nu\ \Delta_f G^0 \tag{11}$$

where ν represents a stoichiometric coefficient [Popovic, 2023a, 2022b, 2022e; Atkins and de Paula, 2011, 2014; von Stockar, 2013a, 2013b; Battley, 1998]. The most important of these three properties is standard Gibbs energy of biosynthesis, which represents the thermodynamic driving force for growth of all organisms [von Stockar, 2013a, 2013b; von Stockar and Liu, 1999], including viruses [Popovic, 2023a, 2022b, 2022e].

3. Results

Genetic and protein sequences were used to find empirical formulas of Zeta P.2, Eta B.1.525, Theta P.3, Kappa B.1.617.1, Iota B.1.526, Lambda C.37 and Mu B.1.621 variants of SARS-CoV-2. This was done through the atom counting method [Popovic, 2022a]. The calculated empirical formulas are shown in Table 1. The empirical formula of the nucleocapsid of Zeta P.2 variant is $CH_{1.573524}O_{0.342720}N_{0.312382}P_{0.006034}S_{0.003358}$. The molar mass of the empirical formula is 23.7501 g/C-mol, while the molar mass of the entire nucleocapsid is 117.228 MDa. The empirical formula of the nucleocapsid of Eta B.1.525 variant is $CH_{1.573539}O_{0.342699}N_{0.312381}$

Table 2
Standard thermodynamic properties of nucleocapsids of SARS-CoV-2 variants. This table shows standard enthalpies of formation, $\Delta_f H°$, standard molar entropies, $S°_m$, and standard Gibbs energies of formation, $\Delta_f G°$.

Name	$\Delta_f H°$ (kJ/C-mol)	$S°_m$ (J/C-mol K)	$\Delta_f G°$ (kJ/C-mol)
Zeta P.2	-75.40	32.49	-33.28
Eta B.1.525	-75.40	32.49	-33.28
Theta P.3	-75.42	32.49	-33.30
Kappa B.1.617.1	-75.41	32.49	-33.29
Iota B.1.526	-75.40	32.49	-33.28
Lambda C.37	-75.41	32.49	-33.29
Mu B.1.621	-75.32	32.49	-33.20

$P_{0.006029}S_{0.003358}$, with the molar mass of the empirical formula is 23.7496 g/C-mol and the molar mass of the entire nucleocapsid of 117.220 MDa. The empirical formula of the Theta P.3 variant nucleocapsid is $CH_{1.573478}O_{0.342775}N_{0.312394}P_{0.006047}S_{0.003358}$, with the molar mass of the empirical formula of 23.7514 g/C-mol and the molar mass of the entire nucleocapsid of 117.251 MDa. The empirical formula of the nucleocapsid of Kappa B.1.617.1 variant is $CH_{1.573509}O_{0.342742}N_{0.312384}P_{0.006038}S_{0.003358}$. The molar mass of the empirical formula is 23.7505 g/C-mol, while the molar mass of the entire nucleocapsid is 117.235 MDa. Iota B.1.526 variant has the empirical formula of the nucleocapsid $CH_{1.573526}O_{0.342719}N_{0.312381}P_{0.006033}S_{0.003358}$. The molar mass of the empirical formula is 23.7500 g/C-mol, while the molar mass of the entire nucleocapsid is 117.227 MDa. The empirical formula of the nucleocapsid of Lambda C.37 variant is $CH_{1.573499}O_{0.342751}N_{0.312387}P_{0.006041}S_{0.003358}$. The molar mass of the empirical formula is 23.7508 g/C-mol, while the molar mass of the entire nucleocapsid is 117.240 MDa. The empirical formula of the nucleocapsid of Mu B.1.621 variant is $CH_{1.573821}O_{0.342372}N_{0.312300}P_{0.005948}S_{0.003361}$. The molar mass of the empirical formula is 23.7410 g/C-mol, while the molar mass of the entire nucleocapsid is 117.081 MDa.

Table 2 shows standard thermodynamic properties of nucleocapsids of Zeta P.2, Eta B.1.525, Theta P.3, Kappa B.1.617.1, Iota B.1.526, Lambda C.37 and Mu B.1.621 variants of SARS-CoV-2. They were calculated based on empirical formulas, through the Patel-Erickson [Patel and Erickson, 1981; Battley, 1998] and Battley models [Battley, 1999a; Battley and Stone, 2000]. For the Zeta P.2 variant nucleocapsid, standard enthalpy of formation is -75.40 kJ/C-mol, standard molar entropy is 32.49 J/C-mol K and standard Gibbs energy of formation is -33.28 kJ/C-mol. For the Eta B.1.525 variant nucleocapsid, standard enthalpy of formation is -75.40 kJ/C-mol, standard molar entropy is 32.49 J/C-mol K and standard Gibbs energy of formation is -33.28 kJ/C-mol. For the Theta P.3 variant nucleocapsid, standard enthalpy of formation is -75.42 kJ/C-mol, standard molar entropy is 32.49 J/C-mol K and standard Gibbs energy of formation is -33.30 kJ/C-mol. For the Kappa B.1.617.1 variant nucleocapsid, standard enthalpy of formation is -75.41 kJ/C-mol, standard molar entropy is 32.49 J/C-mol K and standard Gibbs energy of formation is -33.29 kJ/C-mol. For the Iota B.1.526 variant nucleocapsid, standard enthalpy of formation is -75.40 kJ/C-mol, standard molar entropy is 32.49 J/C-mol K and standard Gibbs energy of formation is -33.28 kJ/C-mol. For the Lambda C.37 variant nucleocapsid, standard enthalpy of formation is -75.41 kJ/C-mol, standard molar entropy is 32.49 J/C-mol K and standard Gibbs energy of formation is -33.29 kJ/C-mol. For the Mu B.1.621 variant nucleocapsid, standard enthalpy of formation is -75.32 kJ/C-mol, standard molar entropy is 32.49 J/C-mol K and standard Gibbs energy of formation is -33.20 kJ/C-mol.

Table 3 shows biosynthesis stoichiometries for the nucleocapsids of Zeta P.2, Eta B.1.525, Theta P.3, Kappa B.1.617.1, Iota B.1.526, Lambda C.37 and Mu B.1.621 variants of SARS-CoV-2. They were calculated based on empirical formulas from Table 1. For the Zeta P.2 variant, the biosynthesis reaction is

$$1.39010CH_{1.798}O_{0.4831}N_{0.2247}S_{0.022472} + 0.49131O_2 + 0.00603HPO_4^{2-} + 0.04369HCO_3^- \rightarrow CH_{1.573524}O_{0.342720}N_{0.312382}P_{0.006034}S_{0.003358} + 0.02788SO_4^{2-} + 0.05384H_2O + 0.43379H_2CO_3 \quad (12)$$

where $CH_{1.798}O_{0.4831}N_{0.2247}S_{0.022472}$ represents a mixture of amino acids and $CH_{1.573524}O_{0.342720}N_{0.312382}P_{0.006034}S_{0.003358}$ is the empirical formula of the Zeta P.2 nucleocapsid (Table 1). For the Eta B.1.525 variant, the biosynthesis reaction is

$$1.39009CH_{1.798}O_{0.4831}N_{0.2247}S_{0.022472} + 0.49129O_2 + 0.00603HPO_4^{2-} + 0.04370HCO_3^- \rightarrow CH_{1.573539}O_{0.342699}N_{0.312381}P_{0.006029}S_{0.003358} + 0.02788SO_4^{2-} + 0.05382H_2O + 0.43380H_2CO_3 \quad (13)$$

where $CH_{1.573539}O_{0.342699}N_{0.312381}P_{0.006029}S_{0.003358}$ represents the empirical formula of the Eta B.1.525 nucleocapsid (Table 1). For the Theta P.3 variant, the biosynthesis reaction is

$$1.39015CH_{1.798}O_{0.4831}N_{0.2247}S_{0.022472} + 0.49140O_2 + 0.00605HPO_4^{2-} + 0.04367HCO_3^- \rightarrow CH_{1.573478}O_{0.342775}N_{0.312394}P_{0.006047}S_{0.003358} + 0.02788SO_4^{2-} + 0.05387H_2O + 0.43382H_2CO_3 \quad (14)$$

where $CH_{1.573478}O_{0.342775}N_{0.312394}P_{0.006047}S_{0.003358}$ is the empirical formulas of the Theta P.3 nucleocapsid (Table 1). For the Kappa B.1.617.1 variant, the biosynthesis reaction is

$$1.39011CH_{1.798}O_{0.4831}N_{0.2247}S_{0.022472} + 0.49133O_2 + 0.00604HPO_4^{2-} + 0.04368HCO_3^- \rightarrow CH_{1.573509}O_{0.342742}N_{0.312384}P_{0.006038}S_{0.003358} + 0.02788SO_4^{2-} + 0.05385H_2O + 0.43379H_2CO_3 \quad (15)$$

Where $CH_{1.573509}O_{0.342742}N_{0.312384}P_{0.006038}S_{0.003358}$ is the empirical formula of the Kappa B.1.617.1 nucleocapsid (Table 1). For the Iota B.1.526 variant, the biosynthesis reaction is

$$1.39009CH_{1.798}O_{0.4831}N_{0.2247}S_{0.022472} + 0.49130O_2 + 0.00603HPO_4^{2-} + 0.04369HCO_3^- \rightarrow CH_{1.573526}O_{0.342719}N_{0.312381}P_{0.006033}S_{0.003358} + 0.02788SO_4^{2-} + 0.05384H_2O + 0.43379H_2CO_3 \quad (16)$$

Where $CH_{1.573526}O_{0.342719}N_{0.312381}P_{0.006033}S_{0.003358}$ is the empirical

Table 3
Biosynthesis reactions of nucleocapsids of SARS-CoV-2 variants. The biosynthesis reactions have the general form (Amino acids) + O_2 + HPO_4^{2-} + HCO_3^- → (Bio) + SO_4^{2-} + H_2O + H_2CO_3, where (Bio) denotes the empirical formula of live matter from Table 1. The stoichiometric coefficients for the biosynthesis reactions are given in this table.

Name	Reactants					Products			
	Amino acid	O_2	HPO_4^{2-}	HCO_3^-	→	Bio	SO_4^{2-}	H_2O	H_2CO_3
Zeta P.2	1.39010	0.49131	0.00603	0.04369	→	1	0.02788	0.05384	0.43379
Eta B.1.525	1.39009	0.49129	0.00603	0.04370	→	1	0.02788	0.05382	0.43380
Theta P.3	1.39015	0.49140	0.00605	0.04367	→	1	0.02788	0.05387	0.43382
Kappa B.1.617.1	1.39011	0.49133	0.00604	0.04368	→	1	0.02788	0.05385	0.43379
Iota B.1.526	1.39009	0.49130	0.00603	0.04369	→	1	0.02788	0.05384	0.43379
Lambda C.37	1.39012	0.49135	0.00604	0.04368	→	1	0.02788	0.05386	0.43380
Mu B.1.621	1.38973	0.49071	0.00595	0.04384	→	1	0.02787	0.05361	0.43358

Table 4
Standard thermodynamic properties of biosynthesis of nucleocapsids of SARS-CoV-2 variants. This table shows standard enthalpies of biosynthesis, $\Delta_{bs}H°$, standard entropies of biosynthesis, $\Delta_{bs}S°$, and standard Gibbs energies of biosynthesis, $\Delta_{bs}G°$.

Name	Δ_{bs}H° (kJ/C-mol)	Δ_{bs}S° (J/C-mol K)	Δ_{bs}G° (kJ/C-mol)
Zeta P.2	-232.35	-37.35	-221.26
Eta B.1.525	-232.34	-37.34	-221.25
Theta P.3	-232.39	-37.35	-221.29
Kappa B.1.617.1	-232.36	-37.35	-221.26
Iota B.1.526	-232.35	-37.34	-221.25
Lambda C.37	-232.37	-37.35	-221.27
Mu B.1.621	-232.09	-37.28	-221.01

formula of the Iota B.1.526 nucleocapsid (Table 1). For the Lambda C.37 variant, the biosynthesis reaction is

$$1.39012CH_{1.798}O_{0.4831}N_{0.2247}S_{0.022472} + 0.49135O_2 + 0.00604HPO_4^{2-} + 0.04368HCO_3^- \rightarrow CH_{1.573499}O_{0.342751}N_{0.312387}P_{0.006041}S_{0.003358} + 0.02788SO_4^{2-} + 0.05386H_2O + 0.43380H_2CO_3 \quad (17)$$

Where $CH_{1.573499}O_{0.342751}N_{0.312387}P_{0.006041}S_{0.003358}$ is the empirical formula of the Lambda C.37 nucleocapsid (Table 1). For the Mu B.1.621 variant, the biosynthesis reaction is

$$1.38973CH_{1.798}O_{0.4831}N_{0.2247}S_{0.022472} + 0.49071O_2 + 0.00595HPO_4^{2-} + 0.04384HCO_3^- \rightarrow CH_{1.573821}O_{0.342372}N_{0.312300}P_{0.005948}S_{0.003361} + 0.02787SO_4^{2-} + 0.05361H_2O + 0.43358H_2CO_3 \quad (18)$$

where $CH_{1.573821}O_{0.342372}N_{0.312300}P_{0.005948}S_{0.003361}$ is the empirical formula of the Mu B.1.621 nucleocapsid (Table 1).

Table 4 gives standard thermodynamic properties of biosynthesis for the Zeta P.2, Eta B.1.525, Theta P.3, Kappa B.1.617.1, Iota B.1.526, Lambda C.37 and Mu B.1.621 variants of SARS-CoV-2. They were calculated by applying the Hess's law [Atkins and de Paula, 2011, 2014] to the biosynthesis reactions from Table 3. For the Zeta P.2 variant, standard enthalpy of biosynthesis is -232.35 kJ/C-mol, standard entropy of biosynthesis is -37.35 J/C-mol K and standard Gibbs energy of biosynthesis is -221.26 kJ/C-mol. For the Eta B.1.525 variant, standard enthalpy of biosynthesis is -232.34 kJ/C-mol, standard entropy of biosynthesis is -37.34 J/C-mol K and standard Gibbs energy of biosynthesis is -221.25 kJ/C-mol. For the Theta P.3 variant, standard enthalpy of biosynthesis is -232.39 kJ/C-mol, standard entropy of biosynthesis is -37.35 J/C-mol K and standard Gibbs energy of biosynthesis is -221.29 kJ/C-mol. For the Kappa B.1.617.1 variant, standard enthalpy of biosynthesis is -232.36 kJ/C-mol, standard entropy of biosynthesis is -37.35 J/C-mol K and standard Gibbs energy of biosynthesis is -221.26 kJ/C-mol. For the Iota B.1.526 variant, standard enthalpy of biosynthesis is -232.35 kJ/C-mol, standard entropy of biosynthesis is -37.34 J/C-mol K and standard Gibbs energy of biosynthesis is -221.25 kJ/C-mol. For the Lambda C.37 variant, standard enthalpy of biosynthesis is -232.37 kJ/C-mol, standard entropy of biosynthesis is -37.35 J/C-mol K and standard Gibbs energy of biosynthesis is -221.27 kJ/C-mol. For the Mu B.1.621 variant, standard enthalpy of biosynthesis is -232.09 kJ/C-mol, standard entropy of biosynthesis is -37.28 J/C-mol K and standard Gibbs energy of biosynthesis is -221.01 kJ/C-mol.

4. Discussion

SARS-CoV-2 belongs to the group of RNA viruses, which exhibit a particular tendency towards acquisition of mutations [Duffy, 2018]. The mutations in SARS-CoV-2 are so frequent that during the 3 years of the pandemic, it acquired several dozen mutations [Thakur et al., 2022; Abavisani et al., 2022; Carabelli et al., 2023; McGrath et al., 2022; Escalera et al., 2022]. Thus, several dozen variants of SARS-CoV-2 have been registered [Fan et al., 2022; Zeyaullah et al., 2021; Gong et al., 2022; Han and Ye, 2022; Mishra et al., 2021]. A great number of variants has been chemically and thermodynamically characterized [Gale, 2022; Şimşek et al., 2021; Popovic, 2023a, 2023b, 2023c, 2022b, 2022c, 2022d, 2022e, 2022f, 2022g, 2022h; Popovic and Minceva, 2022b; Popovic and Popovic, 2022]. However, due to the high frequency of appearance of new mutations, chemical and thermodynamic characterization of particular variants could not be performed during the duration of the pandemic.

During 3.5 years, an intense evolution of SARS-CoV-2 occurred right in front of our eyes [WHO, 2023b; Chen et al., 2021; Jaroszewski et al., 2020; Singh and Yi, 2021; Rochman et al., 2021; González-Vázquez and Arenas, 2023] It was described from the perspective of evolutionary biology [Telenti et al., 2022; Ortiz-Pineda et al., 2022; Ruan et al., 2022] and partly from the perspectives of chemistry and biothermodynamics [Popovic, 2023b, 2022e, 2022k]. In this paper, chemical and thermodynamic properties of the missing puzzles (variants) in virus evolution will be analyzed, to obtain a full insight into the thermodynamic background of evolution of SARS-CoV-2. It is not enough to know the fact that there has been an acquisition of mutations and name the mutations. Knowing only the name of the mutations does not provide us with the mechanism and driving forces for which the mutations occurred. Thermodynamic background (driving force) of all processes in nature is change in Gibbs energy [Demirel, 2014; Balmer, 2010; Atkins and de Paula, 2011, 2014]. The biothermodynamic background of virus host interactions is change in thermodynamic properties of systems and their environment (e.g. enthalpy, entropy and Gibbs energy) [Popovic, 2022b, 2022c, 2022e, 2023b; Popovic and Minceva, 2020a].

Virus-host interactions occur at the host cell membrane and in the cytoplasm [Riedel et al., 2019; Mihaescu et al., 2020; Butnariu et al., 2021; Eskandarzade et al., 2022]. Biothermodynamic background of interactions at the membrane is antigen-receptor binding. Thermodynamic characterization of virus-host interaction is available in the literature [Gale, 2022, 2020, 2019, 2018; Casasnovas and Springer, 1995; Popovic and Popovic, 2022; Popovic, 2022b, 2022c, 2022g, 2022g, 2022h]. SARS-CoV-2 interaction with its host (spike glycoprotein-ACE2 binding) has been reported in the literature [Gale, 2022; Casasnovas and Springer, 1995; Popovic and Popovic, 2022; Popovic, 2022b, 2022c, 2022g, 2022g, 2022h, 2022i, 2022j].

Thermodynamic analysis has shown that SARS-CoV-2 has evolved towards more negative Gibbs energy of binding [Popovic, 2023b, 2022e, 2022k]. This coincides with the observation that mutations have led to an increased antigen-receptor binding affinity and infectivity. These observations are in agreement with the observations of the evolution theory [Popovic, 2023b, 2022e, 2022k]. Negative Gibbs energy was shown to be the driving force for all processes in nature [Demirel, 2014; Balmer, 2010; Atkins and de Paula, 2011, 2014]. Thus, the tendency towards more negative Gibbs energy makes biological evolution a spontaneous process.

Virus-host interaction in the cytoplasm represents the hijacking of cell metabolic machinery [Mayer et al., 2019; Thaker et al., 2019]. Biosynthesis of the building blocks of the host cell and viral components are competitive reactions [Popovic and Minceva, 2020a]. Biosynthesis reactions characterized by more negative Gibbs energy have a competitive advantage [Popovic, 2023a, 2023b, 2023c, 2022e]. More negative Gibbs energy of biosynthesis of viral components, compared to host cell components, enables the hijacking of the cell metabolic machinery and multiplication of viruses [Popovic and Minceva, 2020a]. Thus, we can conclude that thermodynamics has a leading role in interactions of viruses with their hosts [Head et al., 2022; Mahmoudabadi et al., 2017; Rombel-Bryzek et al., 2023; García-Iriepa et al., 2020; Casasnovas and Springer, 1995; Mrevlishvili et al., 1999; Maskow et al., 2010; Guosheng et al., 2003].

Mechanistic models of the evolution theory are available in the literature [Doebeli et al., 2017]. They are necessary for good understanding of the physical processes underlying evolution as a biological process. The process of viral evolution has been analyzed from the

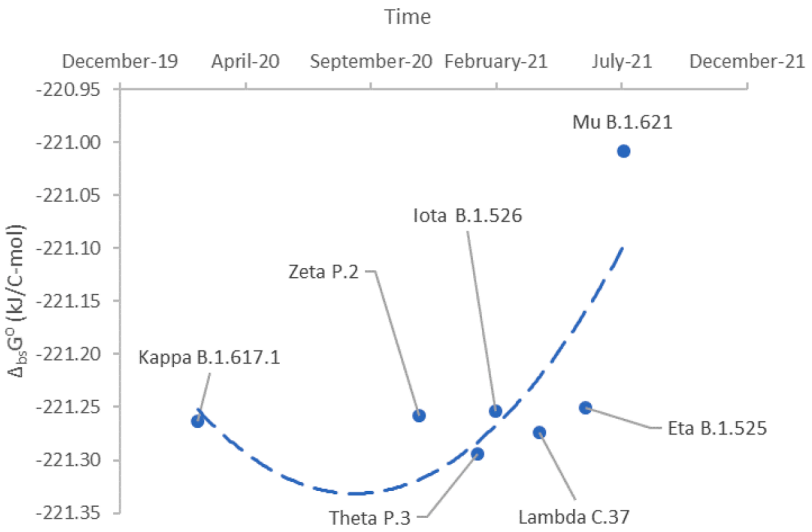

Fig. 1. Gibbs energies of biosynthesis of SARS-CoV-2 variants that dominated in 2020 and early 2021. The line represents a fit with the function: $\Delta_{bs}G^o = (2.2573 \times 10^{-6}$ kJ C-mol^{-1} day$^{-2}) \times t^2 + (-1.2668 \times 10^{-3}$ kJ C-mol^{-1} day$^{-1}) \times t + (-2.2115 \times 10^{+2}$ kJ C-mol^{-1}), where t is time in days since the appearance of the Hu-1 variant.

mechanistic perspective [Ghafari et al., 2021]. To fully understand the evolution process, it is necessary to calculate the driving force that leads to change in state of the system through acquisition of mutations and adaptation of the system to the interaction with the animate and inanimate environment. During evolution, from original Hu-1 to the latest Omicron XBB.1.5, SARS-CoV-2 has acquired mutations. During mutation, there is substitution of nucleotides with different nucleotides and amino acids with different amino acids [Popovic, 2022e]. The replacement of nucleotides and amino acids leads to chemical changes in the system (virion). In particular, due to change in the nucleic acid sequence, there is change in the empirical formula of the newly evolved virus variants. Change in empirical formula causes change in thermodynamic properties. Change in thermodynamic properties causes change in thermodynamic state of the system. The driving force for change in thermodynamic systems is Gibbs energy [von Stockar, 2013a, 2013b; Assael et al., 2022; Demirel, 2014; Atkins and de Paula, 2011, 2014; Popovic, 2022e]. Indeed, changes in Gibbs energy of binding and biosynthesis have been reported in the literature for most SARS-CoV-2 variants [Gale, 2022; Şimşek et al., 2023; Popovic, 2023a, 2023b, 2023c, 2022b, 2022c, 2022d, 2022e, 2022f, 2022g, 2022h, 2022k; Popovic and Popovic, 2022; Popovic and Minceva, 2020b].

Fig. 1 shows changes in Gibbs energies of biosynthesis for the Zeta P.2, Eta B.1.525, Theta P.3, Kappa B.1.617.1, Iota B.1.526, Lambda C.37 and Mu B.1.621 variants of SARS-CoV-2, which have not been reported before in the literature. Gibbs energies for the reported variants exhibit small oscillations except for Mu B.1.621 variant. The trend of change in Gibbs energy is towards less negative Gibbs energy of biosynthesis, mostly due to the Mu B.1.621 variant. From this we can conclude that Gibbs energy during evolution of the mentioned variants has remained constant or became slightly less negative. Since Gibbs energy of biosynthesis influences the multiplication rate, according to the biosynthesis phenomenological equation

$$r_{bs} = -\frac{L_{bs}}{T}\Delta_{bs}G \tag{19}$$

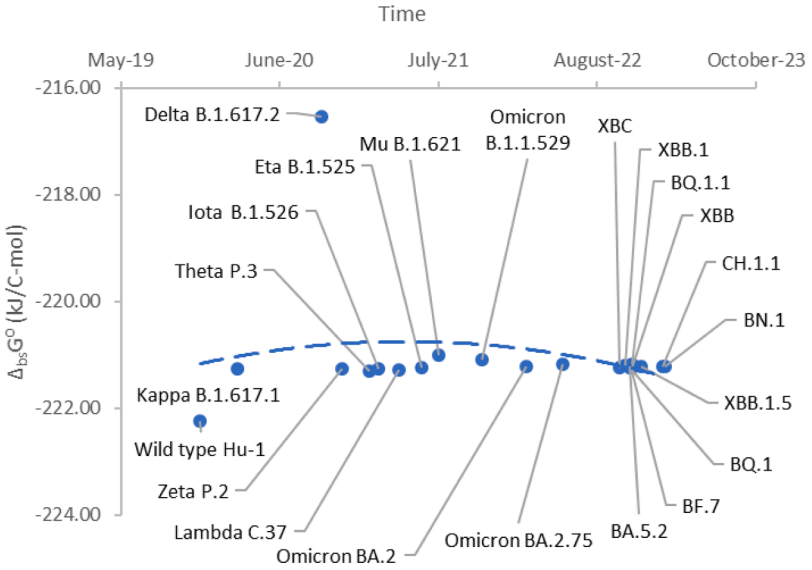

Fig. 2. Gibbs energies of biosynthesis of SARS-CoV-2 variants through evolution: from the wild type Hu-1 variant in late 2019, to the newest Omicron variants. The line represents a fit with the function: $\Delta_{bs}G^o = (-1.5503 \times 10^{-6}$ kJ C-mol^{-1} day$^{-2}) \times t^2 + (1.6059 \times 10^{-3}$ kJ C-mol^{-1} day$^{-1}) \times t + (-2.2117 \times 10^{+2}$ kJ C-mol^{-1}), where t is time in days since the appearance of the Hu-1 variant.

(where L_{bs} is the biosynthesis phenomenological coefficient) it can be expected that the rate of biosynthesis of viral components during evolution of SARS-CoV-2 has stagnated or slightly decreased. Since host cell damage depends on the virus multiplication rate, it would be expected that the pathogenicity and severity of clinical picture have also stagnated or slightly decreased. However, if we analyze only the Gibbs energies of biosynthesis of the variants analyzed in this paper (Fig. 1), we can conclude that Gibbs energy oscillates from -221.01 kJ/C-mol to -221.29 kJ/C-mol. This means that the multiplication rates of viruses change very slightly.

Fig. 2 shows the time evolution of SARS-CoV-2 variants from Hu-1 to the newest Omicron CH.1.1 and BN.1 variants. The figure clearly shows that the most negative Gibbs energy of biosynthesis is that of the Hu-1 variant and that the newer variants have evolved towards less negative Gibbs energy of biosynthesis. Again, less negative Gibbs energy of biosynthesis implies lower rate of synthesis of viral components, which leads to lower damage to host cells. Lower damage to host cells implies a less severe clinical picture. Indeed, Omicron is associated with lower disease severity [Markov et al., 2023; ECDC, 2022].

From Fig. 2 we see that Gibbs energies of biosynthesis of SARS-CoV-2 variants started in late 2019 with Hu-1, which had the lowest Gibbs energy of biosynthesis. Then they slowly increased through the Kappa, Zeta, Theta, Iota, Lambda and Eta variants. Gibbs energy of biosynthesis reached the least negative value with the Delta, Mu and Omicron BA.1 variant in late 2021. After that, it slowly started to become more negative with the Omicron variants. Since the late 2022, Gibbs energy of biosynthesis of the newest Omicron variants has been approximately constant.

This means that the pathogenicity of SARS-CoV-2 was the greatest with the Hu-1 variant. Then it slowly decreased through the Kappa, Zeta, Theta, Iota, Lambda and Eta variants. It became the lowest with the Delta, Mu and Omicron BA.1 variants. Then it started to increase slightly with the Omicron variants and is now constant with the newest Omicron variants.

The fight for survival of every SARS-CoV-2 variant implies a tendency to increase infectivity and rate of spreading, and decrease pathogenicity to preserve the "soil" corps for the virus. This means that the evolution theory predicts increase in infectivity and decrease in pathogenicity. In thermodynamic terminology, a more negative Gibbs energy of binding and less negative Gibbs energy of biosynthesis is predicted. Fig. 2 shows that thermodynamic evolution has really occurred according to the predictions of the biological evolution. Fig. 2 from the paper [Popovic, 2023b] shows change in Gibbs energy of binding during evolution of SARS-CoV-2. Fig. 2 from this paper shows change in Gibbs energy of biosynthesis during evolution of SARS-CoV-2. The results from these two graphs clearly show that the driving forces for evolution of SARS-CoV-2 are Gibbs energy of biosynthesis and Gibbs energy of binding.

Table 1 shows empirical formulas for Zeta P.2, Eta B.1.525, Theta P.3, Kappa B.1.617.1, Iota B.1.526, Lambda C.37 and Mu B.1.621 variants of SARS-CoV-2. Changes in empirical formulas are small (on the second decimal), as a consequence of a small number of mutations in the analyzed variants. Small changes in empirical formulas lead to small changes in thermodynamic properties, which are shown in Table 2. The most pronounced changes in Gibbs energy of formation of nucleocapsid are between Mu B.1.621 and other variants. Changes in molar entropy of nucleocapsids are absent. There are small changes in enthalpies of formation of nucleocapsids.

This paper reports for the first time biosynthesis reactions for the Zeta P.2, Eta B.1.525, Theta P.3, Kappa B.1.617.1, Iota B.1.526, Lambda C.37 and Mu B.1.621 variants of SARS-CoV-2 (Table 3). The stoichiometries of biosynthesis for the analyzed SARS-CoV-2 variants are slightly different, due to differences in empirical formulas.

Table 4 gives thermodynamic properties of biosynthesis, which determine the rate of multiplication of the analyzed SARS-CoV-2 variants. Entropies of biosynthesis are very similar for all the variants, except for the Mu B.1.621 variant. Gibbs energy of biosynthesis (driving force for multiplication of viruses) also deviates for the Mu B.1.621 variant. This implies that the Mu B.1.621 variant has the lowest multiplication potential, compared to the other variants analyzed in this research.

Table 5
Lineages, spike mutations and time of first detection for the Eta, Theta, Kappa, Iota, Zeta, Mu and Lambda variants of SARS-CoV-2. Data taken from [ECDC, 2023].

WHO label	Lineage + additional mutations	Country first detected	Spike mutations of interest	Year and month first detected
Eta	B.1.525	Nigeria	E484K, D614G, Q677H	Dec-20
Theta	P.3	The Philippines	E484K, N501Y, D614G, P681H	Jan-21
Kappa	B.1.617.1	India	L452R, E484Q, D614G, P681R	Dec-20
Iota	B.1.526	USA	E484K, D614G, A701V	Dec-20
Zeta	P.2	Brazil	E484K, D614G	Jan-21
Mu	B.1.621	Colombia	R346K, E484K, N501Y, D614G, P681H	Jan-21
Lambda	C.37	Peru	L452Q, F490S, D614G	Dec-20

Table 5 gives the chronological order of appearance of the analyzed SARS-CoV-2 variants during the evolution of the virus. Evolution of SARS-CoV-2 has continued by acquisition of mutations. The latest variants are XBB.1.9.1, XBF and XBB.1.16 [WHO, 2023c].

5. Conclusion

Chemical and thermodynamic properties have been analyzed for the Zeta P.2, Eta B.1.525, Theta P.3, Kappa B.1.617.1, Iota B.1.526, Lambda C.37 and Mu B.1.621 variants of SARS-CoV-2, for which data could not be found in the literature. Empirical formulas, biosynthesis reactions and thermodynamic properties for the analyzed SARS-CoV-2 variants have been formulated for the first time.

Evolution of SARS-CoV-2 has occurred in accordance with the predictions of the evolution theory, towards increase in infectivity and decrease in pathogenicity. Thermodynamic background of this process is change in Gibbs energy of binding towards more negative and change in Gibbs energy of biosynthesis towards less negative.

Declaration of Competing Interest

None.

Acknowledgements

This work was supported by the Ministry of Science, Technological Development and Innovation of the Republic of Serbia (Grant No. 451-03-47/2023-01/200026).

Supplementary materials

Supplementary material associated with this article can be found, in the online version, at doi:10.1016/j.mran.2023.100263.

References

Abavisani, M., Rahimian, K., Mahdavi, B., Tokhanbigli, S., Mollapour Siasakht, M., Farhadi, A., Kodori, M., Mahmanzar, M., Meshkat, Z., 2022. Mutations in SARS-CoV-2 structural proteins: a global analysis. Virol. J. 19 (1), 220. https://doi.org/10.1186/s12985-022-01951-7.

Assael, M.J., Maitland, G.C., Maskow, T., von Stockar, U., Wakeham, W.A., Will, S., 2022. Commonly Asked Questions in Thermodynamics. CRC Press, Boca Raton, FL. https://doi.org/10.1201/9780429329524, 2nd edISBN: 9780367338916.

Atkins, P.W., de Paula, J., 2011. Physical Chemistry for the Life Sciences. W. H. Freeman and Company, 2nd editionISBN-13: 978-1429231145.

Atkins, P.W., de Paula, J., 2014. Physical Chemistry: Thermodynamics, Structure, and Change. W. H. Freeman and Company, New York, 10th EditionISBN-13: 978-1429290197.

Balmer, R.T., 2010. Modern Engineering Thermodynamics. Academic Press, Cambridge, MA. https://doi.org/10.1016/C2009-0-20199-1.

Battley, E.H., Stone, J.R., 2000. A comparison of values for the entropy and the entropy of formation of selected organic substances of biological importance in the solid state, as determined experimentally or calculated empirically. Thermochim. Acta 349 (1-2), 153–161. https://doi.org/10.1016/S0040-6031(99)00509-2.

Battley, E.H., 2013. A theoretical study of the thermodynamics of microbial growth using Saccharomyces cerevisiae and a different free energy equation. Q. Rev. Biol. 88 (2), 69–96. https://doi.org/10.1086/670529.

Battley, E.H., 1999a. An empirical method for estimating the entropy of formation and the absolute entropy of dried microbial biomass for use in studies on the thermodynamics of microbial growth. Thermochim. Acta 326 (1-2), 7–15. https://doi.org/10.1016/S0040-6031(98)00584-X.

Battley, E.H., 1999b. The thermodynamics of microbial growth. Handbook of Thermal Analysis and Calorimetry. Elsevier, Amsterdam, pp. 219–235. https://doi.org/10.1016/S1573-4374(99)80008-9 vol. 4: From Macromolecules to Man; E.B. Kemp, ed.

Battley, E.H., 1998. The development of direct and indirect methods for the study of the thermodynamics of microbial growth. Thermochim. Acta 309 (1-2), 17–37. https://doi.org/10.1016/S0040-6031(97)00357-2.

Battley, E.H., Putnam, R.L., Boerio-Goates, J., 1997. Heat capacity measurements from 10 to 300 K and derived thermodynamic functions of lyophilized cells of Saccharomyces cerevisiae including the absolute entropy and the entropy of formation at 298.15 K. Thermochim. Acta 298 (1-2), 37–46. https://doi.org/10.1016/S0040-6031(97)00108-1.

Battley, E.H., 1992. On the enthalpy of formation of Escherichia coli K-12 cells. Biotechnol. Bioeng. 39, 5–12. https://doi.org/10.1002/bit.260390103.

Butnariu, A.B., Look, A., Grillo, M., Tabish, T.A., McGarvey, M.J., Pranjol, M.Z.I., 2021. SARS-CoV-2-host cell surface interactions and potential antiviral therapies. Interface Focus 12 (1), 20200081. https://doi.org/10.1098/rsfs.2020.0081.

Carabelli, A. M., Peacock, T. P., Thorne, L. G., Harvey, W. T., Hughes, J., COVID-19 Genomics UK Consortium, Peacock, S. J., Barclay, W. S., de Silva, T. I., Towers, G. J., Robertson, D. L. (2023). SARS-CoV-2 variant biology: immune escape, transmission and fitness. Nat. Rev. Microbiol., 21(3), 162–177. https://doi.org/10.1038/s41579-022-00841-7.

Casasnovas, J.M., Springer, T.A., 1995. Kinetics and thermodynamics of virus binding to receptor: Studies with rhinovirus, intercellular adhesion molecule-1 (ICAM-1), and surface plasmon resonance. J. Biol. Chem. 270 (22), 13216–13224. https://www.doi.org/10.1074/jbc.270.22.13216.

CDC (2023). CDC Museum COVID-19 Timeline [Online] Centers for Disease Control and Prevention, https://www.cdc.gov/museum/timeline/covid19.html (Accessed on March 23, 2023).

Chen, J., Wang, R., & Wei, G. W. (2021). Review of the mechanisms of SARS-CoV-2 evolution and transmission. ArXiv, arXiv:2109.08148v1.

Coudert, E., Gehant, S., de Castro, E., Pozzato, M., Baratin, D., Neto, T., Sigrist, C.J.A., Redaschi, N., Bridge, A., The UniProt Consortium, 2023. Annotation of biologically relevant ligands in UniProtKB using ChEBI. Bioinformatics 39 (1). https://doi.org/10.1093/bioinformatics/btac793. VolumeIssueJanuary 2023, btac793.

Degueldre, C., 2021. Single virus inductively coupled plasma mass spectroscopy analysis: A comprehensive study. Talanta 228, 122211. https://doi.org/10.1016/j.talanta.2021.122211.

Demirel, Y., 2014. Nonequilibrium Thermodynamics: Transport and Rate Processes in Physical, Chemical and Biological Systems. Elsevier, Amsterdam, 3rd edISBN: 9780444595812.

Doebeli, M., Ispolatov, Y., Simon, B., 2017. Towards a mechanistic foundation of evolutionary theory. Elife 6. https://doi.org/10.7554/eLife.23804 e23804.

Duboc, P., Marison, I., Von Stockar, U, 1999. Quantitative calorimetry and biochemical engineering. Handbook of Thermal Analysis and Calorimetry. Elsevier, Amsterdam, pp. 267–365. https://doi.org/10.1016/S1573-4374(99)80009-0 vol. 4: From Macromolecules to Man; E.B. Kemp, ed.

Duffy, S., 2018. Why are RNA virus mutation rates so damn high? PLoS Biol. 16 (8), e3000003 https://doi.org/10.1371/journal.pbio.3000003.

ECDC (2023). SARS-CoV-2 variants of concern as of 20 April 2023 [Online] European Centre for Disease Prevention and Control, https://www.ecdc.europa.eu/en/covid-19/variants-concern (Accessed on May 7, 2023).

ECDC (2022). Assessment of the further spread and potential impact of the SARS-CoV-2 Omicron variant of concern in the EU/EEA, 19th update - 27 January 2022 [Online] European Centre for Disease Prevention and Control, https://www.ecdc.europa.eu/en/publications-data/covid-19-omicron-risk-assessment-further-emergence-and-potential-impact (Accessed on May 7, 2023).

Elbe, S., Buckland-Merrett, G., 2017. Data, disease and diplomacy: GISAID's innovative contribution to global health. Glob. Chall. 1, 33–46. https://doi.org/10.1002/gch2.1018. PMCID: 31565258.

Escalera, A., Gonzalez-Reiche, A.S., Aslam, S., Mena, I., Laporte, M., Pearl, R.L., Fossati, A., Rathnasinghe, R., Alshammary, H., van de Guchte, A., Farrugia, K., Qin, Y., Bouhaddou, M., Kehrer, T., Zuliani-Alvarez, L., Meekins, D.A., Balaraman, V., McDowell, C., Richt, J.A., Bajic, G., …, Aydillo, T., 2022. Mutations in SARS-CoV-2 variants of concern link to increased spike cleavage and virus transmission. Cell Host Microbe 30 (3), 373–387. https://doi.org/10.1016/j.chom.2022.01.006 e7.

Eskandarzade, N., Ghorbani, A., Samarfard, S., Diaz, J., Guzzi, P.H., Fariborzi, N., Tahmasebi, A., Izadpanah, K., 2022. Network for network concept offers new insights into host- SARS-CoV-2 protein interactions and potential novel targets for developing antiviral drugs. Comput. Biol. Med. 146, 105575 https://doi.org/10.1016/j.compbiomed.2022.105575.

Fan, Y., Li, X., Zhang, L., et al., 2022. SARS-CoV-2 Omicron variant: recent progress and future perspectives. Signal Transduction Targeted Ther. 7, 141. https://doi.org/10.1038/s41392-022-00997-x, 2022.

Gale, P., 2022. Using thermodynamic equilibrium models to predict the effect of antiviral agents on infectivity: Theoretical application to SARS-CoV-2 and other viruses. Microb. Risk Anal. 21, 100198 https://doi.org/10.1016/j.mran.2021.100198.

Gale, P., 2020. How virus size and attachment parameters affect the temperature sensitivity of virus binding to host cells: Predictions of a thermodynamic model for arboviruses and HIV. Microb. Risk Anal. 15, 100104 https://doi.org/10.1016/j.mran.2020.100104.

Gale, P., 2019. Towards a thermodynamic mechanistic model for the effect of temperature on arthropod vector competence for transmission of arboviruses. Microb. Risk Anal. 12, 27–43. https://doi.org/10.1016/j.mran.2019.03.001.

Gale, P., 2018. Using thermodynamic parameters to calibrate a mechanistic dose-response for infection of a host by a virus. Microb. Risk Anal. 8, 1–13. https://doi.org/10.1016/j.mran.2018.01.002.

García-Iriepa, C., Hognon, C., Francés-Monerris, A., Iriepa, I., Miclot, T., Barone, G., Monari, A., Marazzi, M., 2020. Thermodynamics of the Interaction between the Spike Protein of Severe Acute Respiratory Syndrome Coronavirus-2 and the Receptor of Human Angiotensin-Converting Enzyme 2. Effects of Possible Ligands. J. Phys. Chem. Lett. 11 (21), 9272–9281. https://doi.org/10.1021/acs.jpclett.0c02203.

Ghafari, M., Simmonds, P., Pybus, O.G., Katzourakis, A., 2021. A mechanistic evolutionary model explains the time-dependent pattern of substitution rates in viruses. Curr. Biol. 31 (21), 4689–4696. https://doi.org/10.1016/j.cub.2021.08.020GISAID e5(2023)GISAID database. [Online] Available at. https://gisaid.org/ (Accessed on March 13, 2023).

Glansdorff, P., Prigogine, I., 1971. Thermodynamic Theory of Structure, Stability and Fluctuations. Wiley, Hoboken, NJ. ISBN-13: 978-0471302803.

Gong, W., Parkkila, S., Wu, X., & Aspatwar, A. (2022). SARS-CoV-2 variants and COVID-19 vaccines: Current challenges and future strategies. International reviews of immunology, 1–22. Advance online publication. https://doi.org/10.1080/08830185.2022.2079642.

González-Vázquez, L.D., Arenas, M., 2023. Molecular Evolution of SARS-CoV-2 during the COVID-19 Pandemic. Genes 14 (2), 407. https://doi.org/10.3390/genes14020407. MDPI AG. Retrieved from.

Guosheng, L., Yi, L., Xiangdong, C., Peng, L., Ping, S., Songsheng, Q., 2003. Study on interaction between T4 phage and Escherichia coli B by microcalorimetric method. J. Virol. Methods 112 (1-2), 137–143. https://doi.org/10.1016/s0166-0934(03)00214-3.

Mihaescu, G., Chifiriuc, M.C., Iliescu, C., Vrancianu, C.O., Ditu, L.M., Marutescu, L.G., Grigore, R., Bertești, Ș., Constantin, M., Gradisteanu Pircalabioru, G., 2020. SARS-CoV-2: From Structure to Pathology, Host Immune Response and Therapeutic Management. Microorganisms 8 (10), 1468. https://doi.org/10.3390/microorganisms8101468.

Han, X., Ye, Q., 2022. The variants of SARS-CoV-2 and the challenges of vaccines. J. Med. Virol. 94 (4), 1366–1372. https://doi.org/10.1002/jmv.27513.

Hansen, L.D., Tolley, H.D., Woodfield, B.F., 2021. Transformation of matter in living organisms during growth and evolution. Biophys. Chem. 271, 106550 https://doi.org/10.1016/j.bpc.2021.106550.

Hansen, L.D., Popovic, M., Tolley, H.D., Woodfield, B.F., 2018. Laws of evolution parallel the laws of thermodynamics. J. Chem. Thermodyn. 124, 141–148. https://doi.org/10.1016/j.jct.2018.05.005.

Hansen, L.D., Criddle, R.S., Battley, E.H., 2009. Biological calorimetry and the thermodynamics of the origination and evolution of life. Pure Appl. Chem. 81 (10), 1843–1855. https://doi.org/10.1351/PAC-CON-08-09-09.

Head, R.J., Lumbers, E.R., Jarrott, B., Tretter, F., Smith, G., Pringle, K.G., Islam, S., Martin, J.H., 2022. Systems analysis shows that thermodynamic physiological and pharmacological fundamentals drive COVID-19 and response to treatment. Pharmacol. Res. Perspect. 10 (1), e00922. https://doi.org/10.1002/prp2.922.

Jackson, C.B., Farzan, M., Chen, B., et al., 2022. Mechanisms of SARS-CoV-2 entry into cells. Nat. Rev. Mol. Cell Biol. 23, 3–20. https://doi.org/10.1038/s41580-021-00418-x.

Jaroszewski, L., Iyer, M., Alisoltani, A., Sedova, M., & Godzik, A. (2020). The interplay of SARS-CoV-2 evolution and constraints imposed by the structure and functionality of its proteins. bioRxiv: the preprint server for biology, 2020.08.10.244756. https://doi.org/10.1101/2020.08.10.244756.

Khare, S., et al., 2021. GISAID's Role in Pandemic Response. China CDC Wkly. 3 (49), 1049–1051. https://doi.org/10.46234/ccdcw2021.255. PMCID: 8668406.

Mahmoudabadi, G., Milo, R., Phillips, R., 2017. Energetic cost of building a virus. Proc. Natl. Acad. Sci. 114 (22), E4324–E4333. https://doi.org/10.1073/pnas.1701670114.

Markov, P.V., Ghafari, M., Beer, M., et al., 2023. The evolution of SARS-CoV-2. Nat Rev Microbiol. https://doi.org/10.1038/s41579-023-00878-2.

Maskow, T., Kiesel, B., Schubert, T., Yong, Z., Harms, H., Yao, J., 2010. Calorimetric real time monitoring of lambda prophage induction. J. Virol. Methods 168 (1-2), 126–132. https://doi.org/10.1016/j.jviromet.2010.05.002.

Mayer, K.A., Stöckl, J., Zlabinger, G.J., Gualdoni, G.A., 2019. Hijacking the Supplies: Metabolism as a Novel Facet of Virus-Host Interaction. Front. Immunol. 10, 1533. https://doi.org/10.3389/fimmu.2019.01533.

McGrath, M.E., Xue, Y., Dillen, C., Oldfield, L., Assad-Garcia, N., Zaveri, J., Singh, N., Baracco, L., Taylor, L.J., Vashee, S., Frieman, M.B., 2022. SARS-CoV-2 variant spike and accessory gene mutations alter pathogenesis. Proc. Nat. Acad. Sci. U.S.A. 119 (37), e2204717119 https://doi.org/10.1073/pnas.2204717119.

Mishra, S., Mindermann, S., Sharma, M., Whittaker, C., Mellan, T.A., Wilton, T., Klapsa, D., Mate, R., Fritzsche, M., Zambon, M., Ahuja, J., Howes, A., Miscouridou, X., Nason, G.P., Ratmann, O., Semenova, E., Leech, G., Sandkühler, J. F., Rogers-Smith, C., Vollmer, M., …, COVID-19 Genomics UK (COG-UK) Consortium, 2021. Changing composition of SARS-CoV-2 lineages and rise of Delta variant in England. EClinicalMedicine 39, 101064. https://doi.org/10.1016/j.eclinm.2021.101064.

Morowitz, H.J., Kostelnik, J.D., Yang, J., Cody, G.D., 2000. The origin of intermediary metabolism. Proc. Natl. Acad. Sci. 97 (14), 7704–7708. https://doi.org/10.1073/pnas.110153997.

Morowitz, H., 1995. The emergence of complexity. Complex 1 (1), 4–5. https://doi.org/10.1002/cplx.6130010102.

Morowitz, H.J., 1992. Beginnings of Cellular Life: Metabolism Recapitulates Biogenesis. Yale University Press, New Haven, CT.

Morowitz, H.J., Heinz, B., Deamer, D.W., 1988. The chemical logic of a minimum protocell. Origins Life Evol Biosphere 18, 281–287. https://doi.org/10.1007/BF01804674.

Morowitz, H.J., 1968. Energy Flow in Biology: Biological Organization as a Problem in Thermal Physics. Academic Press, New York.

Morowitz, H.J., 1955. Some order-disorder considerations in living systems. Bull. Math. Biophys. 17, 81–86. https://doi.org/10.1007/BF02477985.

Mrevlishvili, G.M., Mdzinarashvili, T., Al-Zaza, M., Tsinadze, L., Tushishvili, D., Razmadze, G., 1999. The thermodynamic basis of the mechanisms of bacterial virus infection. Pure Appl. Chem. 71 (7), 1291–1299. https://doi.org/10.1351/pac199971071291.

Müller, I., 2010. A History of Thermodynamics: The Doctrine of Energy and Entropy. Springer, Berlin. ISBN-13: 978-3642079641.

NCBI (2023). NCBI Database [Online]. National Center for Biotechnology Information. Available at: https://www.ncbi.nlm.nih.gov/ (Accessed on March 13, 2023).

Neuman, B.W., Buchmeier, M.J., 2016. Supramolecular architecture of the coronavirus particle. Adv. Virus Res. 96, 1–27. https://doi.org/10.1016/bs.aivir.2016.08.005.

Neuman, B.W., Kiss, G., Kunding, A.H., Bhella, D., Baksh, M.F., Connelly, S., Droese, B., Klaus, J.P., Makino, S., Sawicki, S.G., Siddell, S.G., Stamou, D.G., Wilson, I.A., Kuhn, P., Buchmeier, M.J., 2011. A structural analysis of M protein in coronavirus assembly and morphology. J. Struct. Biol. 174 (1), 11–22. https://doi.org/10.1016/j.jsb.2010.11.021.

Neuman, B.W., Adair, B.D., Yoshioka, C., Quispe, J.D., Orca, G., Kuhn, P., Milligan, R.A., Yeager, M., Buchmeier, M.J., 2006. Supramolecular architecture of severe acute respiratory syndrome coronavirus revealed by electron cryomicroscopy. J. Virol. 80 (16), 7918–7928. https://doi.org/10.1128/JVI.00645-06.

Ortiz-Pineda, P.A., Sierra-Torres, C.H., 2022. Evolutionary Traits and Genomic Surveillance of SARS-CoV-2 in South America. Glob. Health Epidemiol. Genom., 8551576 https://doi.org/10.1155/2022/8551576, 2022.

Overduin, M., Kervin, T.A., Tran, A., 2022. Progressive membrane-binding mechanism of SARS-CoV-2 variant spike proteins. iScience 25 (8), 104722. https://doi.org/10.1016/j.isci.2022.104722.

Patel, S.A., Erickson, L.E., 1981. Estimation of heats of combustion of biomass from elemental analysis using available electron concepts. Biotechnol. Bioeng. 23, 2051–2067. https://doi.org/10.1002/bit.260230910.

Pavan, M., Bassani, D., Sturlese, M., Moro, S., 2022. From the Wuhan-Hu-1 strain to the XD and XE variants: is targeting the SARS-CoV-2 spike protein still a pharmaceutically relevant option against COVID-19? J. Enzyme Inhib. Med. Chem. 37 (1), 1704–1714. https://doi.org/10.1080/14756366.2022.2081847.

Popovic, M., 2023a. XBB.1.5 Kraken cracked: Gibbs energies of binding and biosynthesis of the XBB.1.5 variant of SARS-CoV-2. Microbiol. Res. 270, 127337 https://doi.org/10.1016/j.micres.2023.127337.

Popovic, M., 2023b. Never ending story? Evolution of SARS-CoV-2 monitored through Gibbs energies of biosynthesis and antigen-receptor binding of Omicron BQ.1, BQ.1.1, XBB and XBB.1 variants. Microb. Risk Anal., 100250 https://doi.org/10.1016/j.mran.2023.100250.

Popovic, M., 2023c. The SARS-CoV-2 Hydra, a monster from the 21st century: Thermodynamics of the BA.5.2 and BF.7 variants. Microb. Risk Anal., 100249 https://doi.org/10.1016/j.mran.2023.100249.

Popovic, M.E., 2023d. Thermodynamics of bacteria-phage interactions T4 and Lambda bacteriophages, and E. coli can coexist in natural ecosystems due to the ratio of their Gibbs energies of biosynthesis. Therm. Sci. 27, 411–431. https://doi.org/10.2298/TSCI2301411P, 1 Part A.

Popovic, M., 2023e. Simple but Powerful: Viroids can Hijack their Host Cells' Metabolism due to Greater Gibbs Energy Dissipation. Preprints. https://doi.org/10.20944/preprints202301.0085.v1, 2023010085.

Popovic, M. (2023f). Brief History of Thermodynamic Research on Microorganisms. Preprints, 2023030112. https://doi.org/10.20944/preprints202303.0112.v1.

Popovic, M. and Popovic, M. (2022). Strain Wars: Competitive interactions between SARS-CoV-2 strains are explained by Gibbs energy of antigen-receptor binding. Microbial Risk Analysis. https://doi.org/10.1016/j.mran.2022.100202.

Popovic, M., 2022a. Atom counting method for determining elemental composition of viruses and its applications in biothermodynamics and environmental science. Comput. Biol. Chem. 96, 107621 https://doi.org/10.1016/j.compbiolchem.2022.107621.

Popovic M. (2022b). Strain wars 3: Differences in infectivity and pathogenicity between Delta and Omicron strains of SARS-CoV-2 can be explained by thermodynamic and kinetic parameters of binding and growth. Microbial risk analysis, 100217. Advance online publication. https://doi.org/10.1016/j.mran.2022.100217.

Popovic, M. (2022c). Strain Wars 4 - Darwinian evolution through Gibbs' glasses: Gibbs energies of binding and growth explain evolution of SARS-CoV-2 from Hu-1 to BA.2. Virology. https://doi.org/10.1016/j.virol.2022.08.009.

Popovic, M., 2022d. Omicron BA.2.75 Sublineage (Centaurus) Follows the Expectations of the Evolution Theory: Less Negative Gibbs Energy of Biosynthesis Indicates Decreased Pathogenicity. Microbiol. Res. 13 (4), 937–952. https://doi.org/10.3390/microbiolres13040066. MDPI AG. Retrieved from.

Popovic, M., 2022e. Biothermodynamics of Viruses from Absolute Zero (1950) to Virothermodynamics (2022). Vaccines 10 (12), 2112. https://doi.org/10.3390/vaccines10122112. MDPI AG. Retrieved from.

Popovic, M., 2022f. Strain wars 2: Binding constants, enthalpies, entropies, Gibbs energies and rates of binding of SARS-CoV-2 variants. Virology 570, 35–44. https://doi.org/10.1016/j.virol.2022.03.008.

Popovic, M., 2022g. Strain Wars 5: Gibbs energies of binding of BA.1 through BA.4 variants of SARS-CoV-2. Microbial Risk Analysis. https://doi.org/10.1016/j.mran.2022.100231.

Popovic, M., 2022h. Omicron BA.2.75 Subvariant of SARS-CoV-2 Is Expected to Have the Greatest Infectivity Compared with the Competing BA.2 and BA.5, Due to Most Negative Gibbs Energy of Binding. BioTech 11 (4), 45. https://doi.org/10.3390/biotech11040045. MDPI AG. Retrieved from.

Popovic, M., 2022i. Why doesn't Ebola virus cause pandemics like SARS-CoV-2? Microbial Risk Analysis. https://doi.org/10.1016/j.mran.2022.100236, 100236.

Popovic, M., 2022j. Formulas for death and life: Chemical composition and biothermodynamic properties of Monkeypox (MPV, MPXV, HMPXV) and Vaccinia (VACV) viruses. Therm. Sci. 26 (6A) https://doi.org/10.2298/TSCI220524142P.

Popovic, M., 2022k. Beyond COVID-19: Do biothermodynamic properties allow predicting the future evolution of SARS-CoV-2 variants? Microb. Risk Anal. 22, 100232 https://doi.org/10.1016/j.mran.2022.100232.

Popovic, M., Stenning, G., Göttlein, A., Minceva, M., 2021. Elemental composition, heat capacity from 2 to 300 K and derived thermodynamic functions of 5 microorganism species. J. Biotechnol. 331, 99–107. https://doi.org/10.1016/j.jbiotec.2021.03.006.

Popovic, M., Minceva, M., 2021a. Coinfection and Interference Phenomena Are the Results of Multiple Thermodynamic Competitive Interactions. Microorganisms 9 (10), 2060. https://doi.org/10.3390/microorganisms9102060.

Popovic, M., Minceva, M., 2020a. A thermodynamic insight into viral infections: do viruses in a lytic cycle hijack cell metabolism due to their low Gibbs energy? Heliyon 6 (5), e03933. https://doi.org/10.1016/j.heliyon.2020 e03933.

Popovic, M., Minceva, M., 2020b. Thermodynamic insight into viral infections 2: empirical formulas, molecular compositions and thermodynamic properties of SARS, MERS and SARS-CoV-2 (COVID-19) viruses. Heliyon 6 (9), e04943. https://doi.org/10.1016/2Fj.heliyon.2020.e04943.

Popovic, M.E., Minceva, M., 2020c. Thermodynamic properties of human tissues. Therm. Sci. 24, 4115–4133. https://doi.org/10.2298/TSCI200109151P, 6 Part B.

Popovic, M., 2018. Living organisms from Prigogine's perspective: an opportunity to introduce students to biological entropy balance. J. Biol. Educ. 52 (3), 294–300. https://doi.org/10.1080/00219266.2017.1357649.

Prigogine, I., Wiame, J.M., 1946. Biologie et thermodynamique des phénomènes irréversibles. Experientia 2, 451–453. https://doi.org/10.1007/BF02153597.

Prigogine, I. (1977). Nobel lecture: Time, Structure and Fluctuations. [Online] Available at: https://www.nobelprize.org/prizes/chemistry/1977/prigogine/lecture/, (Accessed on: January 5, 2023).

Prigogine I. (1947). Etude thermodynamique des phénomènes irréversibles. Paris: Dunod. WorldCat ID: 421502786.

Riedel, S., Hobden, J.A., Miller, S., Morse, S.A., Mietzner, T.A., Detrick, B., Mitchell, T.G., Sakanari, J.A., Hotez, P., Mejia, R., 2019. Jawetz, Melnick and Adelberg's Medical Microbiology. McGraw-Hill, New York, 28th ed.ISBN-13: 978-1260012026.

Rochman, N.D., Wolf, Y.I., Faure, G., Mutz, P., Zhang, F., Koonin, E.V., 2021. Ongoing global and regional adaptive evolution of SARS-CoV-2. Proc. Nat. Acad. Sci. U.S.A. 118 (29), e2104241118 https://doi.org/10.1073/pnas.2104241118.

Rombel-Bryzek, A., Miller, A., Witkowska, D., 2023. Thermodynamic analysis of the interactions between human ACE2 and spike RBD of Betacoronaviruses (SARS-CoV-1 and SARS-CoV-2). FEBS Open Bio. 13 (1), 174–184. https://doi.org/10.1002/2211-5463.13525.

Ruan, Y., Hou, M., Tang, X., He, X., Lu, X., Lu, J., Wu, C.I., Wen, H., 2022. The Runaway Evolution of SARS-CoV-2 Leading to the Highly Evolved Delta Strain. Mol. Biol. Evol. 39 (3) https://doi.org/10.1093/molbev/msac046 msac046.

Sayers, E.W., Bolton, E.E., Brister, J.R., Canese, K., Chan, J., Comeau, D.C., Connor, R., Funk, K., Kelly, C., Kim, S., Madej, T., Marchler-Bauer, A., Lanczycki, C., Lathrop, S., Lu, Z., Thibaud-Nissen, F., Murphy, T., Phan, L., Skripchenko, Y., Tse, T., …, Sherry, S.T., 2022. Database resources of the national center for biotechnology information. Nucleic Acids Res. 50 (D1), D20–D26. https://doi.org/10.1093/nar/gkab1112.

Schrödinger, E., 1944. What is life? The physical aspect of the living cell. Cambridge university press, Cambridge. ISBN: 0-521-42708-8.

Telenti, A., Hodcroft, E.B., Robertson, D.L., 2022. The Evolution and Biology of SARS-CoV-2 Variants. Cold Spring Harb. Perspect. Med. 12 (5) https://doi.org/10.1101/cshperspect.a041390 a041390.

Thaker, S.K., Ch'ng, J., Christofk, H.R., 2019. Viral hijacking of cellular metabolism. BMC Biol. 17 (1), 59. https://doi.org/10.1186/s12915-019-0678-9.

Thakur, S., Sasi, S., Pillai, S.G., Nag, A., Shukla, D., Singhal, R., Phalke, S., Velu, G.S.K., 2022. SARS-CoV-2 Mutations and Their Impact on Diagnostics, Therapeutics and Vaccines. Front. Med. 9, 815389 https://doi.org/10.3389/fmed.2022.815389.

Shu, Y., McCauley, J., 2017. GISAID: from vision to reality. Euro Surveill. 22 (13) https://doi.org/10.2807/1560-7917.ES.2017.22.13.30494. PMCID: PMC5388101.

Şimşek, B., Özilgen, M., & Utku, F. Ş. (2021). How much energy is stored in SARS-CoV-2 and its structural elements?. Energy Storage, e298. https://doi.org/10.1002/est2.298.

Singh, D., Yi, S.V., 2021. On the origin and evolution of SARS-CoV-2. Exp. Mol. Med. 53, 537–547. https://doi.org/10.1038/s12276-021-00604-z.

Skene, K., 2015. Life's a Gas: A Thermodynamic Theory of Biological Evolution. Entropy 17 (12), 5522–5548. https://doi.org/10.3390/e17085522. MDPI AG. Retrieved from.

The UniProt Consortium (2023). UniProt: the Universal Protein Knowledgebase in 2023, Nucleic Acids Research, Volume 51, Issue D1, 6 January 2023, Pages D523–D531, https://doi.org/10.1093/nar/gkac1052.

UniProt (2023). UniProt database [Online] Available at: https://www.uniprot.org/ (Accessed on March 13, 2023).

Von Bertalanffy, L., 1950. The theory of open systems in physics and biology. Science 111 (2872), 23–29. https://doi.org/10.1126/science.111.2872.23.

Von Bertalanffy, L., 1971. General System Theory: Foundations, Development, Applications. George Braziller Inc, New York, NY. ISBN-13: 978-0807604533.

Von Stockar, U. (2013a). Live cells as open non-equilibrium systems. In Urs von Stockar, ed., Biothermodynamics: The Role of Thermodynamics in Biochemical Engineering, Lausanne: EPFL Press, 475-534. https://doi.org/10.1201/b15428.

Von Stockar, U. (2013b). Biothermodynamics of live cells: energy dissipation and heat generation in cellular structures. In: Biothermodynamics: the role of thermodynamics in Biochemical Engineering, von Stockar, U., ed., Lausanne: EPFL Press, pp. 475-534. https://doi.org/10.1201/b15428.

Wang, Y., Wang, Q., Huang, H., Huang, W., Chen, Y., McGarvey, P.B., Wu, C.H., Arighi, C.N., UniProt Consortium, 2021. A crowdsourcing open platform for literature curation in UniProt. PLoS Biol. 19 (12), e3001464 https://doi.org/10.1371/journal.pbio.3001464.

WHO (2023a). WHO Coronavirus (COVID-19) Dashboard [Online] Available at: https://covid19.who.int/ (Accessed on March 13, 2023).

WHO (2023b). Coronavirus disease (COVID-19): Virus Evolution [Online] Available at: https://www.who.int/news-room/questions-and-answers/item/sars-cov-2-evolution (Accessed on March 19, 2023).

WHO (2023c). Tracking SARS-CoV-2 variants [Online] World Health Organization. Available at: https://www.who.int/activities/tracking-SARS-CoV-2-variants (Accessed on May 7, 2023).

Wu, Y.C., Chen, C.S., Chan, Y.J., 2020. The outbreak of COVID-19: An overview. J. Chin. Med. Assoc. 83 (3), 217–220. https://doi.org/10.1097/JCMA.0000000000000270.

Xie, Y., Du, D., Karki, C.B., Guo, W., Lopez-Hernandez, A.E., Sun, S., Juarez, B.Y., Li, H., Wang, J., Li, L., 2020. Revealing the mechanism of SARS-CoV-2 spike protein binding with ACE2. Comput. Sci. Eng. 22 (6), 21–29. https://doi.org/10.1109/MCSE.2020.3015511.

Zeyaullah, M., AlShahrani, A.M., Muzammil, K., Ahmad, I., Alam, S., Khan, W.H., Ahmad, R., 2021. COVID-19 and SARS-CoV-2 Variants: Current Challenges and Health Concern. Front. Genet. 12, 693916 https://doi.org/10.3389/fgene.2021.693916.

Zhang, Z.-B., Xia, Y.-L., Shen, J.-X., Du, W.-W., Fu, Y.-X., Liu, S.-Q., 2022. Mechanistic Origin of Different Binding Affinities of SARS-CoV and SARS-CoV-2 Spike RBDs to Human ACE2. Cells 11 (8), 1274. https://doi.org/10.3390/cells11081274. MDPI AG. Retrieved from.

Zhang, Q., Xiang, R., Huo, S., Zhou, Y., Jiang, S., Wang, Q., Yu, F., 2021. Molecular mechanism of interaction between SARS-CoV-2 and host cells and interventional therapy. Signal Transduction Targeted Ther. 6 (1), 233. https://doi.org/10.1038/s41392-021-00653-w.